


ORIGINAL ARTICLE

Isopropyl-phloroglucinol-DHA protects outer retinal cells against lethal dose of all-*trans*-retinal

Aurélie Cubizolle^{1,2} | David Cia³ | Espérance Moine⁴ | Nathalie Jacquemot³ | Laurent Guillou^{1,2} | Mélissa Rosell⁴ | Claire Angebault-Prouteau^{2,5} | Guy Lenaers⁶ | Isabelle Meunier^{1,7} | Joseph Vercauteren⁴ | Thierry Durand⁴ | Céline Crauste⁴ | Philippe Brabet^{1,2} 

¹INSERM U1051, Institut des Neurosciences de Montpellier, Montpellier, France

²Université Montpellier, Montpellier, France

³UMR INSERM 1107, Laboratoire de Biophysique Neurosensorielle, Facultés de Médecine et de Pharmacie, Clermont-Ferrand, France

⁴UMR5247-CNRS-UM ENSCM Faculté de Pharmacie, Institut des Biomolécules Max Mousseron (IBMM), Montpellier, France

⁵INSERM U1046, UMR CNRS 9214, CHRU de Montpellier, Montpellier, France

⁶INSERM U1083, CNRS UMR 6015, MitoVasc-MitoLab, Université d'Angers, Angers, France

⁷National Reference Centre for Inherited Sensory Disorders, CHU, Montpellier, France

Correspondence

Philippe Brabet, INSERM U1051, Institut des Neurosciences de Montpellier, CHU Saint-Eloi, 80 rue Augustin Fliche, Montpellier 34295, France.

Email: philippe.brabet@inserm.fr

Funding information

Fondation Stargardt / RETINA FRANCE, Grant/Award Number: 2017-03

Abstract

All-*trans*-retinal (atRAL) is a highly reactive carbonyl specie, known for its reactivity on cellular phosphatidylethanolamine in photoreceptor. It is generated by photoisomerization of 11-*cis*-retinal chromophore linked to opsin by the Schiff's base reaction. In ABCA4-associated autosomal recessive Stargardt macular dystrophy, atRAL results in carbonyl and oxidative stress, which leads to bisretinoid A2E, accumulation in the retinal pigment epithelium (RPE). This A2E-accumulation presents as lipofuscin fluorescent pigment, and its photooxidation causes subsequent damage. Here we describe protection against a lethal dose of atRAL in both photoreceptors and RPE in primary cultures by a lipidic polyphenol derivative, an isopropyl-phloroglucinol linked to DHA, referred to as IP-DHA. Next, we addressed the cellular and molecular defence mechanisms in commonly used human ARPE-19 cells. We determined that both polyunsaturated fatty acid and isopropyl substituents bond to phloroglucinol are essential to confer the highest protection. IP-DHA responds rapidly against the toxicity of atRAL and its protective effect persists. This healthy effect of IP-DHA applies to the mitochondrial respiration. IP-DHA also rescues RPE cells subjected to the toxic effects of A2E after blue light exposure. Together, our findings suggest that the beneficial role of IP-DHA in retinal cells involves both anti-carbonyl and anti-oxidative capacities.

KEYWORDS

all-*trans*-retinal, bisretinoid A2E, carbonyl stress, isopropyl-phloroglucinol-DHA conjugate, outer retina cells, oxidative stress

1 | INTRODUCTION

In vertebrates, visual perception occurs in the rod and cone photoreceptor outer segments (POS) through visual pigments, G protein-coupled receptors (rhodopsin and cone opsins) consisting of

the apoprotein opsin and a prosthetic group, the vitamin A-derived chromophore 11-*cis*-retinal (11cRAL).¹ The light isomerizes 11cRAL to *trans* configuration (atRAL) and subsequently elicits the conformational transition within the opsin proteins, followed by the activation of the phototransduction cascade. After photoisomerization of

This is an open access article under the terms of the Creative Commons Attribution License, which permits use, distribution and reproduction in any medium, provided the original work is properly cited.

© 2020 The Authors. Journal of Cellular and Molecular Medicine published by John Wiley & Sons Ltd and Foundation for Cellular and Molecular Medicine.

11cRAL to atRAL in POS, the atRAL Schiff base is hydrolysed, yielding the photochemically inactive opsin protein and the freed atRAL.² Removal of the latter is required to avoid acute toxicity, and delayed clearance of atRAL after light exposure contributes to light-induced retinal degeneration.³ The atRAL is cleared from disc membranes of POS by retinal ATP-binding cassette (ABCA4) transporter proteins to the cytoplasm where atRAL-dehydrogenase (RDH) catalyses its reduction to the much less reactive all-*trans*-retinol (atROL). Mutations in the ABCA4 gene are found in patients with Stargardt macular dystrophy (STGD1), cone-rod dystrophy and recessive retinitis pigmentosa, and variants in ABCA4 increased susceptibility to age-related macular degeneration (AMD).⁴

Mechanisms of acute toxicity of atRAL were previously studied by Palczewski and coworkers.^{3,5} They first reported that NADPH oxidase at the plasma membrane can be activated by an increase in atRAL levels via the phospholipase C/ inositol 1,4,5-triphosphate pathway, resulting in overproduction of reactive oxygen species (ROS). The respiratory chain in mitochondria also participates in ROS production (the more reactive being HO[•]) within the cell in reply to atRAL accumulation.³ More recently, atRAL has been shown to induce mitochondrial transmembrane potential loss and endoplasmic reticulum (ER) stress that ultimately trigger programmed cell death by activating apoptotic Bax- and caspase-dependent cascades.^{6,7} Free atRAL is itself a reactive carbonyl compound through its all-*trans*-polyene conjugated aldehyde that is toxic to cells.^{8,9}

In ABCA4-associated pathologies, atRAL accumulates due to delayed clearance by the defective ABCR transporter. Nickell et al¹⁰ reported that rhodopsin is present at a concentration of 4.62 mmol/L in disc membranes of rod outer segments. Therefore, the level of atRAL released after photoactivation of rhodopsin can range from 25 to 100 $\mu\text{mol/L}$ in the disc membranes following photobleaching of only 0.5%-2%. This level of atRAL is toxic in cultured retinal cells.^{7,9} Excess atRAL is a potent photosensitizer which can mediate light-induced oxidation.¹¹ However, atRAL condenses on the PE by a double mechanism of carbonyl and oxidative stress.^{12,13} This leads to decrease atRAL levels and to the formation of bisretinoid adducts such as A2E and RAL dimer, which are pigments of retinal pigment epithelium (RPE) autofluorescent lipofuscin.¹⁴ These pigments are sensitive to visible blue light and are photo-oxidized and fragmented accordingly.¹⁵ The oxidized metabolites are reactive carbonyl and oxidative species that would have toxic effects in the RPE.¹⁶

Based on epidemiology studies, natural antioxidants such as polyphenols appear as efficient protectors against oxidative stress. This activity may be related to their capacity to block the formation and accumulation of ROS or to stimulate the enzymatic antioxidant defences of the organism.¹⁷ Literature also addressed the efficiency of polyphenols to act as anti-carbonyl stressor agents by trapping reactive toxic carbonyl entities.¹⁸ We previously reported in vitro cytoprotective effects of the polyphenol phloroglucinol, a natural monomer of phlorotannins abundantly present in *Ecklonia cava* (edible brown algae), in outer retinal cells by scavenging ROS and trapping atRAL.⁹ Because of its low bioavailability, phloroglucinol was

then structurally modified by the addition of polyunsaturated fatty acid (PUFA) and isopropyl substituents.¹³

In the present study, we investigated the protective effect of the medicinal chemical compound, isopropyl-phloroglucinol-DHA (IP-DHA), also called lipophenol, against atRAL-related carbonyl and oxidative stresses (COS). We first analysed primary cultures of outer retina to demonstrate the dose-dependent protective effect against lethal dose of atRAL. We then used ARPE-19 cells as a standard cellular model to study the mechanisms of cell death and protection. We demonstrate that each of the structural part, that is isopropyl and PUFA, is essential for the full action of the lipophenol with selectivity for LA and DHA. We compared the capacities of phloroglucinol and IP-DHA to reverse the effects of atRAL and finally discuss how to understand the enhanced protective effects of IP-DHA compared to phloroglucinol.

2 | MATERIALS AND METHODS

2.1 | Chemicals

All-*trans* retinal (atRAL), 3-(4,5-dimethylthiazol-2-yl)-2, 5-diphenyl tetrazolium bromide (MTT) and 2',7'-dichlorofluorescein diacetate (H₂DCFDA) were purchased from Sigma-Aldrich. AtRAL was dissolved in dimethylformamide (DMF) and freshly diluted in serum-free culture medium to working concentrations in 0.1% DMF. MTT and H₂DCFDA were used at 0.5 mg/mL and 2 $\mu\text{mol/L}$, respectively. A2E was synthesized as previously described.¹⁹

2.2 | Synthesis of phloroglucinol lipophenols

To evaluate the influence of different lipid chains and of the isopropyl substituent, several lipophenols were synthesized: five lipophenols with an isopropyl-phloroglucinol (IP) core linked to various fatty acid, IP-DHA, IP-EPA, IP-ALA, IP-LA and IP-C22, and three lipophenols using only the phloroglucinol without alkyl substituent, P-DHA, P-EPA and P-LA. All the lipophenols were synthesized according to the chemical strategy developed by Crauste et al.¹³ Briefly, one hydroxyl group of the phloroglucinol or IP is protected by triisopropylsilyl (TIPS) groups using triflate reagent (TIPS-OTf) and diisopropylethylamine (DIPEA) as a base to obtain the protected derivative. The coupling reactions between the protected polyphenol and the different fatty acids, docosahexaenoic acid (DHA), eicosapentaenoic acid (EPA), α -linolenic acid (ALA), linoleic acid (LA) and behenic acid (C22), were initiated using dicyclohexylcarbodiimide and dimethylaminopyridine (DCC/DMAP) as coupling reagents to access the protected lipophenols. Deprotection of the TIPS groups by Et₃N-3HF in dry tetrahydrofuran (THF) yielded final lipophenols compounds, IP-DHA, IP-EPA, IP-ALA, IP-LA, IP-C22, P-DHA, P-EPA and P-LA. A quality control assessment was established by a complete ¹H and ¹³C NMR spectral analysis for each synthesized

compound (chemical structure, general procedure, yield and NMR analysis are reported in Supporting Information).

2.3 | Cell cultures and atRAL treatment

Primary rat RPE and mouse neural retina (NR) cultures were obtained as previously described.⁹ RPE cells were cultured for 3 days until they reached 80%–85% confluency, and NR was cultured for 10 days until glial cells were confluent in the bottom layer and neural cells with a neurite outgrowth in the upper layer. Human RPE-like cells, ARPE-19, were seeded at 100 000 cells/cm² and grown to confluency before being assayed as instructed by ATCC.

Pre- and co-treatment procedures with lipophenol were carried out. During pre-treatments, rat RPE primary cultures received a medium containing lipophenol at different concentrations (40–320 µmol/L) for 24 hours. The medium was then removed and replaced by a serum-free culture medium containing 25 µmol/L atRAL for 4 hours. During co-treatments, RPE and NR cells received a serum-free medium containing 25 µmol/L atRAL and/or IP-DHA (10–320 µmol/L) for 4 hours. NR cells were refreshed with serum-free medium the next day.

2.4 | A2E treatment

ARPE-19 cells were plated into 96-well plates (4 × 10⁴ cells/well) and cultured for 24 hours to confluence prior to lipophenol treatment. The cell cultures were treated with serum-free DMEM/F12 medium without phenol red containing IP-DHA at different concentrations (0–80 µmol/L) for 1 hour. A2E was then added to a final concentration of 20 µmol/L for 6 hours before rinsing with medium. Control cells were incubated with 0.2% DMSO with or without A2E. The cells were exposed to intense blue light (4600 lux) for 30 minutes to induce phototoxicity of A2E and incubated at 37°C. Irradiation was achieved using a LED device with blue emission wavelengths from 430 to 470 nm and a dimmable luminance (Roleadro lighting). Control ambient white light was less than 300 lux. Without blue light exposure, A2E-loaded cell survival was not affected. The cell viability was determined 16–20 hours later using a MTT colorimetric assay. Results are expressed in percentage of viable cells normalized to control conditions in the absence of lipophenol and stressor.

2.5 | Cell viability

Cell viability in primary RPE and ARPE-19 was determined by MTT assay in 96-well plates as described.⁹ To distinguish viable cells from apoptotic and necrotic cells, treated ARPE-19 were cultured in 24-well plates and stained with Annexin V (A)–FITC and propidium iodide (PI). Cells were analysed by a BD-LSRII flow cytometer with FACSDiva Software (BD Biosciences) at the Cellular Health Imaging Center of Clermont Auvergne University. Living cells were first

sorted according to their size (FSC) and granularity (SSC). Cell states were identified as follow: living cells (A–, PI–), early apoptotic cells (A+, PI–) and late apoptotic/necrotic cells (A+, PI+).

2.6 | Mitochondrial respirometry

Mitochondrial respiration was measured in ARPE-19 cultured in six-well plates after 4-hour exposure to 25 µmol/L atRAL and/or 40 µmol/L lipophenol. Respiration was measured on 10⁶ cells permeabilized by incubation for 2 minutes with 15 µg digitonin and resuspended in a respiratory buffer (pH 7.4, 10 mmol/L KH₂PO₄, 300 mmol/L mannitol, 10 mmol/L KCl and 5 mmol/L MgCl₂). The respiratory rates were recorded at 37°C in 2-mL glass chambers using a high-resolution Oxygraph respirometer (Oroboros) as recently described.²⁰ Assays were initiated in the presence of 5 mmol/L malate/pyruvate to measure basal respiration. (state 2), Complex I-coupled state 3 respiration was measured by adding 0.5 mmol/L NAD⁺/1.5 mmol/L ADP. Then, 10 mmol/L succinate was added to reach maximal coupled respiration, and 10 µmol/L rotenone was injected to obtain the CII-coupled state 3 respiration. Oligomycin (8 µg/mL) was added to determine the uncoupled state 4 respiration rate. Finally, carbonyl cyanide-4-(trifluoromethoxy) phenylhydrazone (1 µmol/L) was added to control the permeabilization of the tissues.

The respiration rate driven by complex IV was measured starting from CII-coupled state 3 and the addition of antimycin A (1 µmol/L), which inhibited complex III, and of ascorbate/TMPD redox couple to reduce cytochrome c.

2.7 | Mitochondrial enzymatic activities

The enzymatic activity of the mitochondrial respiratory chain complexes (RCC) was measured on cell homogenates as described previously.²¹ Briefly, ARPE-19 was grown in six-well plates and treated for 4 hours with 25 µmol/L atRAL and/or 40 µmol/L lipophenol. Cells were scraped, rinsed with DPBS and resuspended on ice with cell buffer (250 mmol/L saccharose, 20 mmol/L tris[hydroxymethyl]aminomethane, 2 mmol/L EGTA, and 1 mg/mL bovine serum albumin (BSA), pH 7.2). Cell was disrupted by two freezing-thawing cycles, centrifuged at 16 000 g for one minute and suspended in the cell buffer (50 µL/10⁶ cells). The cellular protein content was determined with the Bicinchoninic assay kit (Pierce) using BSA as standard. The initial kinetics of enzymatic activities were monitored by spectrophotometry (UV-SAFAS spectrophotometer, SAFAS monaco). Complex I (NADH ubiquinone reductase) activity was measured as described elsewhere²² and adapted using 2, 6 dichloroindophenol (DCPIP) to avoid inhibition of complex I activity by decylubiquinol.²³ Complex II (succinate ubiquinone reductase) activity was measured according to James et al.²⁴ Specific enzymatic activities of complexes I and II were expressed in mIU (ie nanomoles of DCPIP/min/mg protein). Complex IV (cytochrome c oxidase) activity was recorded according

to a method by Rustin et al,²⁵ adapted in a 50 mmol/L KH_2PO_4 buffer, using 15 $\mu\text{mol/L}$ reduced cytochrome *c*. Specific enzymatic activity was expressed in mIU (ie nanomoles of cyt *c*/min/mg protein). Citrate synthase activity was assayed using a standard procedure.²⁶ Specific enzymatic activity was expressed in mIU (ie nanomoles of 5-5'-dithiobis (2-nitrobenzoic acid), DTNB/min/mg protein).

2.8 | ROS production

ROS were measured in ARPE-19 using the H_2DCFDA probe as described⁹ with minor modifications. Radicals such as peroxy, alkoxy, $\text{NO}_2\cdot$, carbonate or $\text{HO}\cdot$ are able to oxidize H_2DCFDA and thus to be quantified by this assay.^{14,27} Briefly, cells seeded on black, optically clear-bottom 96-well plates (Perkin-Elmer) were incubated with 2 $\mu\text{mol/L}$ H_2DCFDA in phenol red free DMEM/F12 for 45 minutes, washed with PBS and then treated by 25 $\mu\text{mol/L}$ atRAL and/or 80 $\mu\text{mol/L}$ lipophenol for 4 hours. Fluorescence intensity was measured immediately by fluorescence assay in 96-well plates using CLARIOstar[®] microplate reader (BMG LABTECH). All experiments were done in quintuple and repeated four times independently.

2.9 | Catalase activity

ARPE-19 cells were seeded in six-well plates and treated as aforementioned. Immediately after treatment, cells were scrapped on ice, centrifuged 5 minutes at 400 g and suspended in 100 μL of PBS. For lysis, cells were sonicated 3 \times 15 seconds, centrifuged 5 minutes at 14 000 g at 4°C and kept on ice. A solution of 0.037% of H_2O_2 was prepared. In a spectrophotometer cuvette, 50 μL of sample was added to 1.45 mL of 0.037% H_2O_2 and reading of an OD at 240 nm every 20 seconds for 15 minutes to determine the quantity of degraded H_2O_2 . Data were expressed in nmol of H_2O_2 degraded/min/mg of protein.

2.10 | GSH/GSSG assay

The levels of GSH and GSSG were measured in ARPE-19 cells plated on tissue culture-treated white-with-clear-bottom 96-well plates using the GSH/GSSG-Glo[™] Assay Kit (Promega V6611) according to the manufacturer's instructions. All experiments were performed in triplicate and repeated three times independently.

2.11 | Western blot analysis

ARPE-19 cells were lysed in RIPA buffer containing protease inhibitors, homogenized and then centrifuged at 9600 g for 3 minutes. Twenty-five micrograms of the protein lysates in Laemmli buffer were separated on 10% SDS-PAGE (Mini-PROTEAN[®] TGX[™] gels, Bio-Rad) and electrotransferred to PVDF membranes (Trans-Blot[®]

Turbo[™] Transfer System, Bio-Rad). After blocking, membranes were blotted overnight at 4°C with primary antibodies. After incubation with the corresponding HRP-conjugated secondary antibodies, detection was performed using an enhanced chemiluminescence kit (Pierce ECL, Thermo Scientific) and recorded by the V3 Western Workflow[™] system (Bio-Rad). The bands were semi-quantified using densitometry by ImageJ software. Commercial antibodies were used to assess protein expression as follows: monoclonal mouse anti-GAPDH (Sigma-Aldrich[®], G8795 diluted to 1:5000, 37 kD); mouse anti- α -tubulin (Sigma-Aldrich[®] T5168, diluted to 1:4000, 55 kD); rabbit anti-cleaved Caspase 3 (Cell Signaling TECHNOLOGY 9661, diluted to 1:200, 17-19 kD); VDAC (Abcam ab14734, diluted to 1:2500, 32 kD); monoclonal rabbit anti-catalase (Cell Signaling TECHNOLOGY 12980, diluted at 1:1000, 60 kD); and monoclonal mouse anti-NQO1 (Cell Signaling TECHNOLOGY 3187, diluted to 1:1000, 29 kD).

2.12 | Immunofluorescence studies

Mouse NR primary cells or ARPE-19 cells were fixed in 4% paraformaldehyde for 10 minutes at room temperature (RT), permeabilized in 0.1% triton for 10 minutes at RT, saturated 20 minutes in 0.1% SDS + 10% donkey serum in PBS for 20 minutes at RT and incubated overnight at 4°C with either mouse monoclonal anti-Rhodopsin antibody RET-P1 (Novus Biologicals[®], NBP120-3267 diluted to 1:500) or rabbit monoclonal anti-Nrf2 antibody (clone D1Z9C, ref: 12721; Cell Signaling TECHNOLOGY[®] diluted at 1:200), and detected with Alexa594-conjugated anti-rabbit or Alexa488-conjugated anti-rabbit secondary antibodies, respectively. Confocal imaging of Rhodopsin and Nrf2 translocation to the nucleus was performed with a Zeiss LSM 5 LIVE DUO Highspeed/ Spectral Confocal system. Image acquisitions were obtained with the Zeiss Zen software.

2.13 | XCELLigence assay

The xCELLigence system (Roche and ACEA Biosciences) was used to monitor cell adhesion, proliferation and cytotoxicity. The xCELLigence system was connected and tested by Resistor Plate before the RTCA Single Plate station was placed inside the incubator at 37°C and 5% CO_2 . First, the optimal seeding concentration for the proliferation experiments of the ARPE-19 cells was determined (30 000 cells/well). After seeding of the required number of cells in 100 μL medium per well of a 16-well E-plate, the attachment, proliferation and spreading of the cells was monitored every 15 minutes by the xCELLigence system. Approximately 16 hours post-seeding, when cells were at subconfluency, they were exposed to atRAL 25 $\mu\text{mol/L}$ and/or IP-DHA 40 $\mu\text{mol/L}$ at the indicated times. Evaluations were performed using xCELLigence 1.2.1 software (Roche and ACEA Biosciences). The real-time impedance traces were reported using a unitless parameter called Cell Index (CI), where $\text{CI} = (\text{impedance at time } n - \text{impedance in the absence of cells}) / \text{nominal impedance value}$.

The experiments were performed using the ARPEGE Pharmacology Screening-Interactome platform facility at the Institute of Functional Genomics.

2.14 | Statistics

Statistical analyses were performed using GraphPad Prism 5.0. Software. Data were first analysed with Shapiro-Wilk normality test, and then, two-tailed *P*-values were determined using either the unpaired Student's *t* test or the non-parametric Mann-Whitney test. A *P*-value < .05 was considered significant. The linear correlation was measured by Pearson's *r* correlation coefficient.

3 | RESULTS

3.1 | IP-DHA protects retinal primary cultures against atRAL toxicity

ABCA4-associated retinopathies often affect both photoreceptor and RPE in a manner that is not fully elucidated,^{5,14} but which originally involves a defective retinal clearance from the photoreceptor. We tested the protection with IP-DHA of atRAL-challenged primary cultures of rat RPE (Figure 1A,B) and mouse NR enriched in photoreceptor cells (Figure 1C). These analyses confirmed significant protective effects of IP-DHA against atRAL, regardless of the mode of treatment (pre- vs co-treatment Figure 1A,B), the density (Figure 1BB1, BB2), or the cell type (RPE and photoreceptor, Figure 1A,B,C). Furthermore, IP-DHA did not show cytotoxicity on the primary RPE at a concentration of 320 $\mu\text{mol/L}$ up to eight times higher than the one we previously reported using the ARPE-19 cell line.¹³ Thus, IP-DHA is able to protect both RPE and photoreceptor from the toxic effects of atRAL overload without adverse effect.

3.2 | Structure-function relationship of IP-DHA

A selection of fatty acids (ω -6, ω -3 and saturated fatty acids) that were conjugated to IP showed a structural selectivity for protection efficacy of ARPE-19 cells challenged with a toxic dose of atRAL (Figure 2A). The rank of efficacy was LA \geq DHA > EPA = ALA > C22. This order was not correlated with the level of fatty acid unsaturation (DHA > EPA > ALA > LA > C22), nor with the rank of the toxicity of free fatty acid (EPA > DHA > ALA > LA > C22, Figure 2B). As oxidation levels are correlated with cell toxicity, PUFA toxicity may come from lipid peroxidation.²⁸ However, coupling polyunsaturated FA (PUFA) to IP or phloroglucinol (P) significantly reduced PUFA toxicity (Figure 2C,D, respectively). These data highlight that isopropyl does not alter the low toxicity of lipophenols. Regardless of the fatty acid, isopropyl function was necessary for effective protection, the protective effect was lost upon use of non-alkylated lipophenols

(P-fatty acid, Figure 2E). These results demonstrated that both PUFA and isopropyl are essential for lipophenol activity.

The choice to use IP-DHA throughout this study rather than IP-LA, despite the latter's showing better protection against atRAL is justified in view of planned *in vivo* evaluations. DHA has general and specific transporters to concentrate DHA in the photoreceptors. Therefore, the use of DHA seems more appropriate to improve the uptake of IP-DHA by the retina. In addition, an ω -3 such as DHA, which can be released by the enzyme esterase, can have beneficial effects on human retinal diseases that ω -6, known for their superior pro-inflammatory properties, cannot reproduce.

3.3 | Cell-based assays of IP-DHA protection

Dynamic cellular biology was first monitored using the xCELLigence System in ARPE-19 before and after treatment with atRAL and/or IP-DHA. The system measures electrical impedance which provides quantitative information about the biological status of the cells, including cell number, viability and morphology. The xCELLigence read-out is a dimensionless parameter called Cell Index (CI) that was normalized with the time-point before the treatment ~16.5 hours after plating (Figure S1). The addition of 25 $\mu\text{mol/L}$ atRAL significantly decreased the CI, which then stabilized 4 hours later at $11 \pm 2\%$ (Figure S1; Table S1). Co-incubation with 40 $\mu\text{mol/L}$ IP-DHA limited this decrease to $56 \pm 11\%$ two hours after the beginning of treatment, and this effect lasted throughout the analysis (37 hours). We conclude that IP-DHA responds rapidly against the toxicity of atRAL with persisting protective effect.

Consequently, we applied a 4-hour co-treatment with atRAL and IP-DHA to assess the protection against detrimental effects induced by atRAL overload in ARPE-19 (Figure 3). As shown in Figure 3A,B, $94.2 \pm 1.7\%$ untreated and $90.1 \pm 4.4\%$ IP-DHA-treated cells survived respectively, suggesting no adverse effect of IP-DHA. Twenty-five $\mu\text{mol/L}$ atRAL reduced cell survival to $54.1 \pm 14.2\%$ by apoptosis and $40.9 \pm 12.5\%$ by necrosis whereas co-incubation with 40 $\mu\text{mol/L}$ IP-DHA significantly increased the living cells to $81.2 \pm 9.9\%$, and reduced necrotic cells to $16.3 \pm 8.4\%$. The absolute values generated by the flow cytometry experiments were higher than those of xCELLigence. The difference between the protocols (toxicity of atRAL) and the measured parameters may be one explanation. It can be assumed that the ARPE-19 cells lose their adhesion but are still alive. Nevertheless, both cellular tests show a similar trend on the survival capacity of ARPE-19 cells co-treated with atRAL and IP-DHA compared to atRAL.

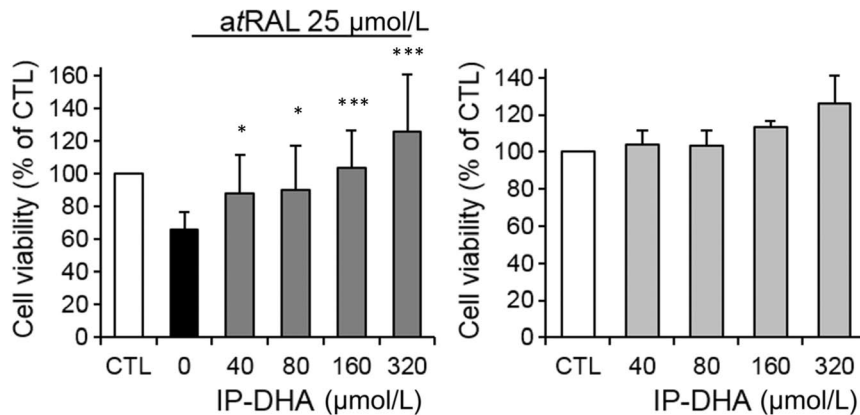
Morphologic changes in ARPE-19 cells were observed following atRAL exposure (Figure 3C) and an apoptotic caspase 3-cleavage signal was detected by Western blot (Figure 3D,E). Long (24 hour's pre-) and short (4-hour co-) IP-DHA treatment restored healthy morphology and abolished the caspase-dependent apoptosis. Previous reports revealed that atRAL could directly act on and elicit a poisonous effect in mitochondria.^{3,7} We therefore performed respirometry to assess the functionality of mitochondrial RCC (Figure 4A). Respiration

Rat retinal pigment epithelium

A Pre-treatment

a1 Protection against atRAL

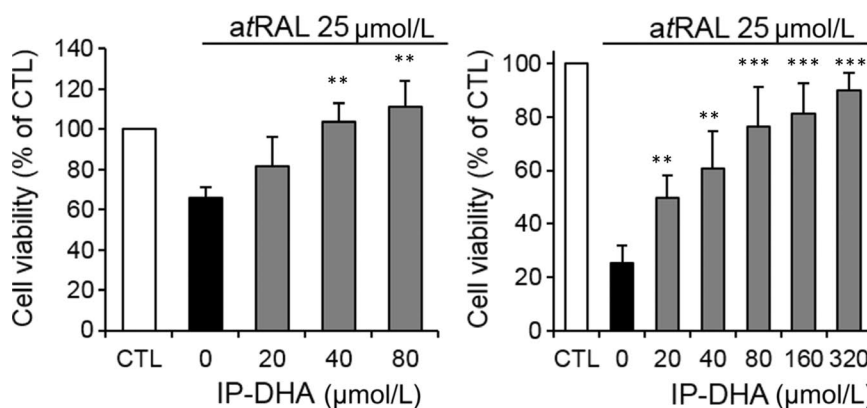
a2 Toxicity of IP-DHA



B Co-treatment

b1 Sub-confluent RPE

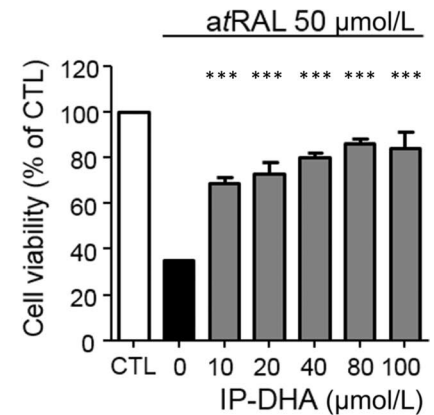
b2 Low-density RPE



Mouse neural retina

c Long-lasting effect

c1 Neural Retina



c2 Rhodopsin-IR cells

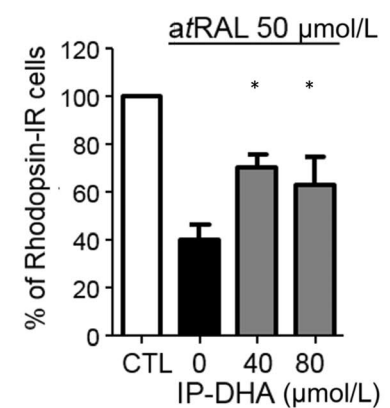


FIGURE 1 Protection of retinal primary cultures by IP-DHA against atRAL. A, pre-treatment of RPE cells with IP-DHA inhibits atRAL-induced cell death. A1, rat primary RPE cells were cultured in 96-well plates and pre-treated with increasing concentrations of IP-DHA for 24 h, washed and exposed to 25 µmol/L atRAL for 4 h. A2, RPE cultures were incubated for 24 h with increasing concentrations of IP-DHA. Cell viability was determined by MTT assay. The data are represented as mean \pm SD ($n = 7$). B, co-treatment with IP-DHA and atRAL protects RPE cells. Sub-confluent (B1) and low-density (twofold less) (B2) cultures of rat primary RPE cells were cultured in 96-well plates and co-incubated with increasing concentrations of IP-DHA and 25 µmol/L atRAL for 4 h. Cell viability was determined by MTT assay. The data are represented as mean \pm SD ($n = 3-6$). C, long-lasting effect of atRAL and IP-DHA on NR and photoreceptors. NR primary cultures were incubated with increasing concentrations of IP-DHA for 1 h, and 50 µmol/L atRAL was added for an additional 4 h. The medium was refreshed for the next 20 h. MTT assay measured cell survival (C1) and Rhodopsin-IR (rhodopsin-immunoreactivity positive cells) revealed the number of photoreceptor-derived primary cells (C2). The data are presented as mean \pm SEM ($n = 3-4$). All data are expressed as a percentage of untreated cells (CTL) * $P < .05$, ** $P < .01$, *** $P < .001$ vs atRAL-treated cells

driven by complexes I, II and IV was evaluated. All responses were dramatically diminished by atRAL treatment. IP-DHA co-treatment partially but significantly rescued the functionality of the mitochondrial respiratory chain. Notably, the constant expression of VDAC (Figure 4B), a major protein of the outer mitochondrial membrane, suggested that atRAL does not induce loss of the mitochondrial mass. Moreover, direct measurement of enzymatic activities clearly showed that all RCC were impaired by atRAL and partially rescued by IP-DHA treatment (Figure 4C). Thus, the protective effect of IP-DHA

seems to apply directly to the mitochondrial respiration essential to the cell viability.

3.4 | Molecular and cellular mechanisms of IP-DHA protection

Natural polyphenols were reported as potent against COS involved in age-related diseases,²⁹ either as sequestering agents of

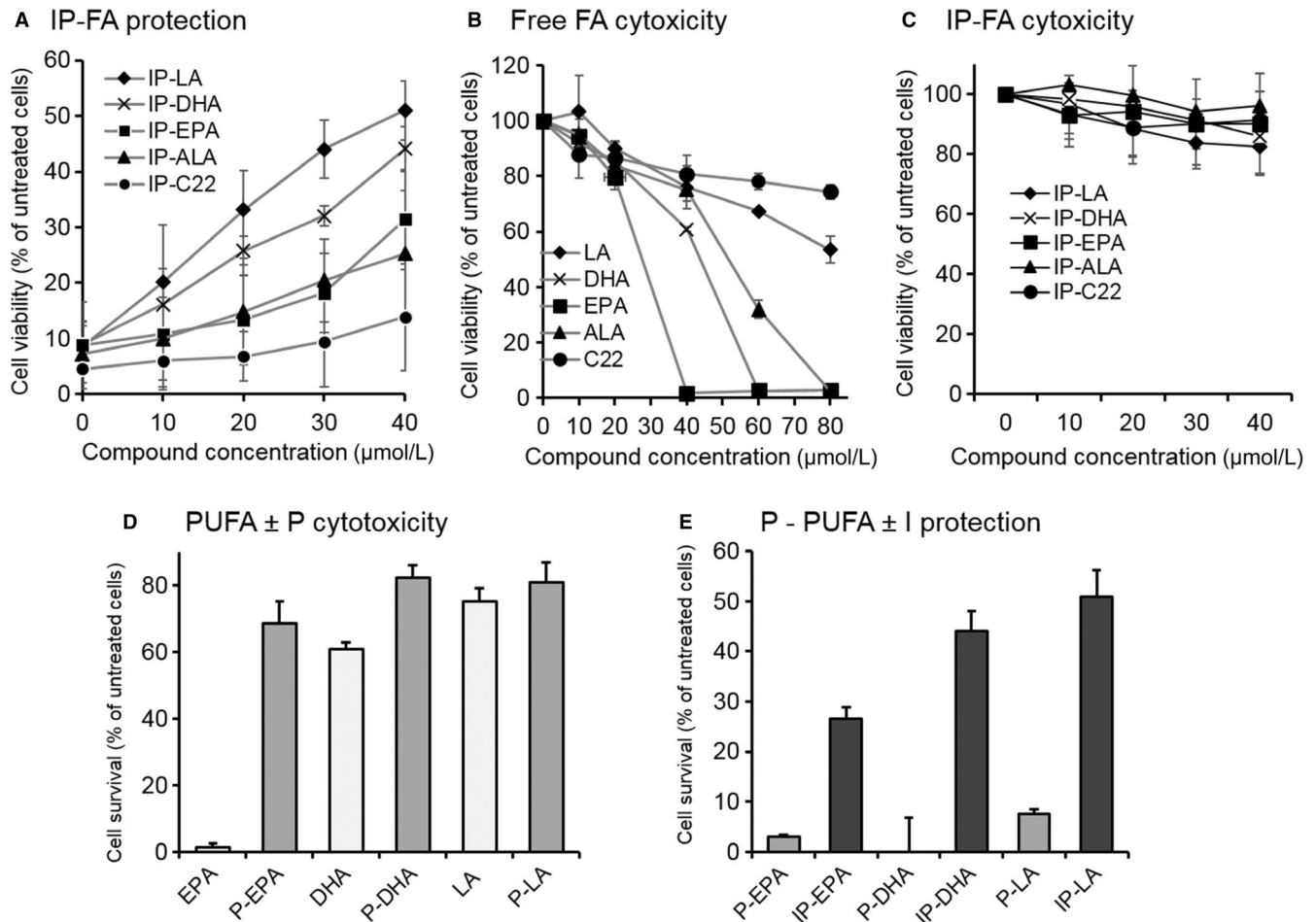


FIGURE 2 Significance of fatty acid and isopropyl for lipophenol toxicity and protection of ARPE-19 against atRAL. A, selective protection by IP fatty acid conjugates (IP-FA). ARPE-19 cells were cultured in 96-well plates and incubated with lipophenols (10–40 μmol/L) for 1 h, and atRAL (25 μmol/L) was added for 4 h co-incubation. Culture medium was changed, and cell viability was determined 16–20 h later by MTT assay. Bars indicate SD of the mean ($n \geq 5$). Cytotoxicity effects of free fatty acid (B) and of IP-FA (C). ARPE-19 cells were incubated with different concentrations for 24 h, and cell viability was determined by MTT assay. PUFA concentrations were selected according to Liu et al.⁴⁸ Bars indicate SD of the mean ($n = 4$ –10). D, E, Significance of phloroglucinol (P) and isopropyl radical (I). Polyunsaturated fatty acid (PUFA) and P-PUFA conjugates (40 μmol/L) were compared for their cytotoxicity on ARPE-19 cells for 24 h (D). P-PUFA (40 μmol/L) was also compared to IP-PUFA (40 μmol/L) for their efficacies to protect ARPE-19 from atRAL-induced cell death (E). Cell viability was determined by MTT assay. Bars indicate SD of the means ($n = 3$). All data are expressed as a percentage of untreated cells. P, phloroglucinol; IP, isopropyl-phloroglucinol; LA, linoleic acid (C18:2 ω6); ALA, linolenic acid (C18:3 ω3); EPA, eicosapentaenoic acid (C20:5 ω3); DHA, docosahexaenoic acid (C22:6 ω3); and C22 (saturated)

reactive aldehydes and scavengers of reactive species, or by the activation of Nrf2 transcription factor that promotes expression of many phase II detoxifying enzymes.³⁰ We recently showed that phloroglucinol acts as an anti-COS agent trapping atRAL and scavenging ROS produced by H₂O₂ treatment (identified by DCFDA probes.^{9,27} Here, we consider the anti-COS capacity of IP-DHA compared to phloroglucinol in RPE cells (Figure 5). IP-DHA reduced both free atRAL and ROS produced by atRAL treatment (Figure 5A and 5B, respectively). AtRAL treatment is able to alter the respiratory chain in mitochondria and potentially disrupts homeostasis in the ER, thereby initiating ER stress, which in turn induces ROS generation such as O₂^{•-} and then HO[•].³¹ IP-DHA was effective in reducing the concentration of free atRAL (Figure 5A) at doses that provided partial (40 μmol/L IP-DHA, 87.0 ± 4.4% of control free

atRAL) and total (320 μmol/L IP-DHA, 81.6 ± 3.7% of control free atRAL) protection of primary rat RPE challenged with 25 μmol/L atRAL. As we previously described,⁹ 400 μmol/L (50 μg/mL) phloroglucinol was most efficient (Figure 5A, 51.3 ± 4.6% of control free atRAL). On the other hand, the two compounds were equipotent for decreasing atRAL-mediated ROS production (Figure 5B). Together, our observations suggest that reducing excess atRAL and oxidative stress status may account for the protective effect of lipophenols on RPE cells.

Besides their scavenging potency, anti-COS compounds also were described as inducers of phase II antioxidant and detoxifying enzymes, which contribute efficiently to the redox homeostasis and prevent retinal cell death both in vivo and in vitro.^{30,32} Activation of the EpRE enzymes through Nrf2/Keap1 pathway

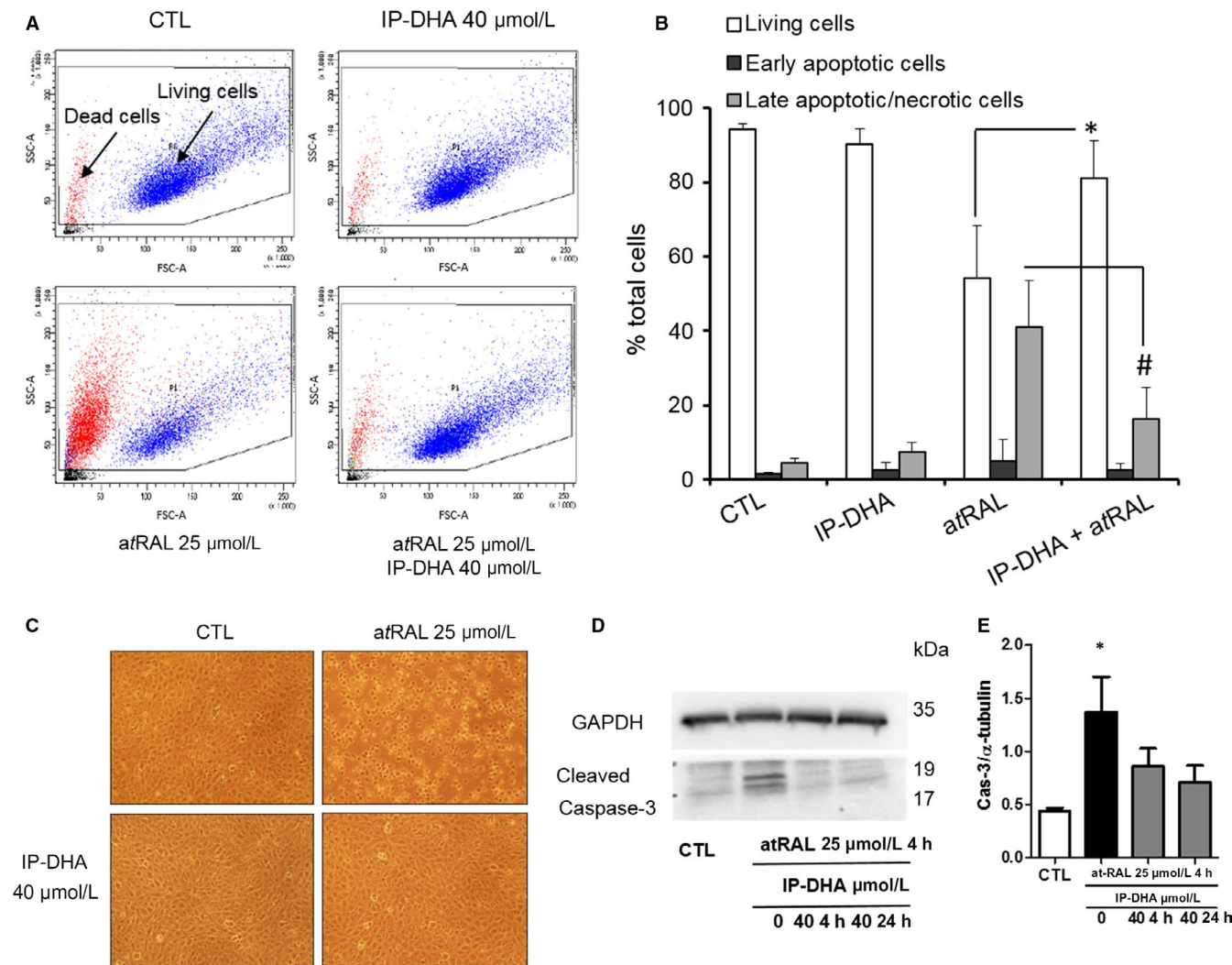


FIGURE 3 IP-DHA markedly reduced atRAL-induced ARPE-19 cell death. A–E ARPE-19 cells were cultured in 24-well plates and co-treated for 4 h with 40 μ mol/L IP-DHA and/or 25 μ mol/L atRAL. To assess cell death, ARPE-19 cells were stained with annexin V-FITC (A) and propidium iodide (PI) and analysed by flow cytometry (A, B). A, living cells are sorted according to their size (FSC) and granularity (SSC). CTL indicates untreated cells. B, the cell populations were identified as follows: living cells (A⁻, PI⁻, white squares), early apoptotic cells (A⁺, PI⁻, black squares) and late apoptotic/necrotic cells (A⁺, PI⁺, grey squares). Results are expressed as a percentage of total cells and presented as mean \pm SD (n = 3). C, Photographs show a preservation of ARPE-19 morphology with 40 μ mol/L IP-DHA even in the presence of 25 μ mol/L atRAL. D and E, ARPE-19 cells showed significantly increased caspase 3 cleavage activity after treatment for 4 h with 25 μ mol/L atRAL (n = 3). This activity in IP-DHA pre-treated (24 h) and co-treated (4 h) cells did not show significant changes when compared to each other or with the untreated cells (CTL)

activation is one of the mechanism of polyphenol antioxidant activity. We measured the activity and expression of key enzymes in defence of the retina, including catalase, glutathione related enzymes and NAD(P)H quinone oxidoreductase (NQO-1; Figure 6). A 4-hour treatment with IP-DHA increased the catalase activity and prevented its decrease by atRAL (Figure 6A), whereas it did not regulate its expression (Figure 6B). The 24 hours pre-treatment with IP-DHA increased in a dose-dependent manner the expression of Nrf2 and its nuclear translocation in ARPE-19 cells (Figure 6C). The same treatment increased the GSH/GSSG ratio (Figure 6D) and the expression of NQO-1 (Figure 6E), suggesting an up-regulation of redox regulating and detoxifying enzymes.

These results support the notion that the protective role of IP-DHA in retinal cells involves both molecular (atRAL reduction) and cellular (enzymatic) mechanisms.

3.5 | IP-DHA rescues cells under toxic effect of blue light-exposed A2E

The daily shedding of the distal tips of the outer segment followed by their phagocytosis in RPE cells leads to accumulation of bisretinoids in lysosomes and formation of A2E.³³ A2E is a pigment which captures blue light and produces reactive carbonyl and oxygen

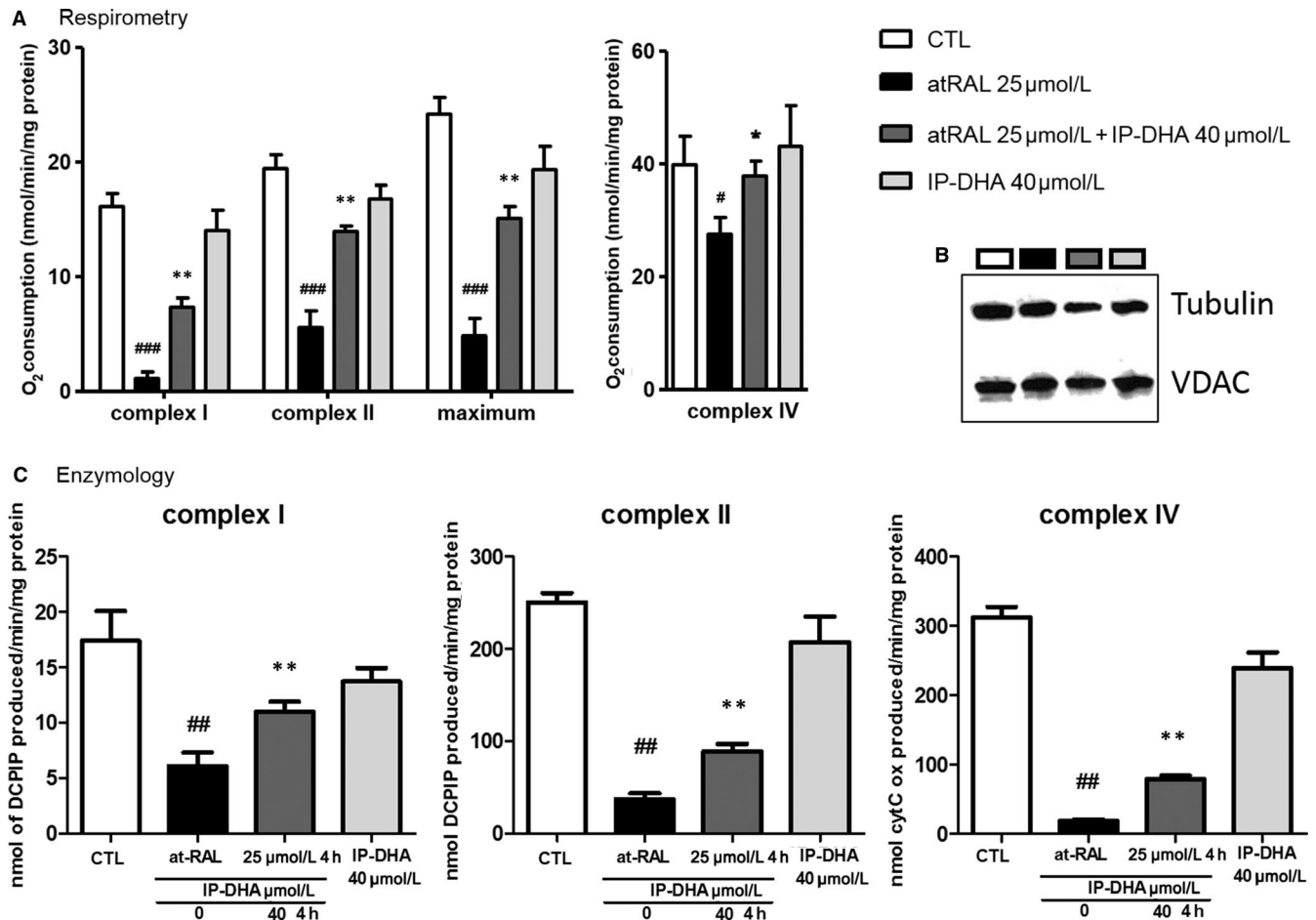


FIGURE 4 The mitochondrial poisoning by atRAL is partially rescued by IP-DHA in ARPE-19. A and B, mitochondrial poisoning by atRAL is partially rescued by IP-DHA. Respirometry estimates the rates of oxygen consumption which is governed by the mitochondrial respiratory complex chain. The respiration driven by (A) and enzymatic activities of (C) complexes I, II and IV were severely affected by 25 $\mu\text{mol/L}$ atRAL but co-treatment with IP-DHA (40 $\mu\text{mol/L}$) significantly rescues both parameters. Results are expressed as means \pm SEM ($n \geq 4$). B, mitochondrial mass was not affected by treatment as demonstrated by a constant immunodetection of VDAC (outer mitochondrial membrane ion channel). # $P < .05$, ## $P < .01$, ### $P < .001$ vs untreated CTL, and * $P < .05$, ** $P < .01$, *** $P < .001$ vs atRAL-treated cells

species that can lead to cell death. We tested whether IP-DHA may inhibit the photo-induced toxic effect of A2E in ARPE-19 cells (Figure 7). The latter were incubated with 20 $\mu\text{mol/L}$ pure synthetic A2E for 6 hours following the addition of IP-DHA at various concentrations for 1 hour. Medium was replaced, and cells were exposed to blue light (430–470 nm, 4600 lux) for 30 minutes before they were returned to the incubator at 37°C overnight. Cell survival analysis using a MTT assay showed that IP-DHA dose-dependently recovers survival from A2E-treated cells. At 80 $\mu\text{mol/L}$, IP-DHA treatment markedly increases cell survival by fourfold.

4 | DISCUSSION

The pathophysiological mechanisms of STGD1, first involve alterations in the photoreceptors due to mutations in the ATP-binding cassette transporter ABCA4 gene, delay in atRAL reduction, and accumulation of autofluorescent bisretinoids in photoreceptors by condensation of atRAL and phosphatidylethanolamine.³⁴ At this

stage, atRAL reactivity is responsible for COS.^{9,13} Later, phagocytosis transfers bisretinoid-burdened POS to the RPE where bisretinoids can account for autofluorescence of lipofuscin, light-dependent COS and consequently death of RPE.³³ Therefore, COS play a crucial role throughout the disease from its onset in the photoreceptors to its progression in the RPE. Thus, it is highly relevant to develop new therapeutic compounds capable of limiting COS in the outer retina.

Polyphenols have long been recognized as antioxidant and more recently as anti-carbonyl stress derivatives, and their application in the treatment of neurodegenerative diseases has been widely acknowledged in the past few years.^{35,36} Among them, phloroglucinol is a monomer of phlorotannins, which also displays therapeutic potential for neurodegenerative diseases.^{37,38} Neurodegeneration is a multifactorial process and polyphenols present pleiotropic effects (antioxidant, anti-inflammatory, immunomodulatory properties) due to their ability to modulate the activity of multiple targets involved in pathogenesis, thereby halting the progression of these diseases. We previously reported cytoprotective effects of phloroglucinol in

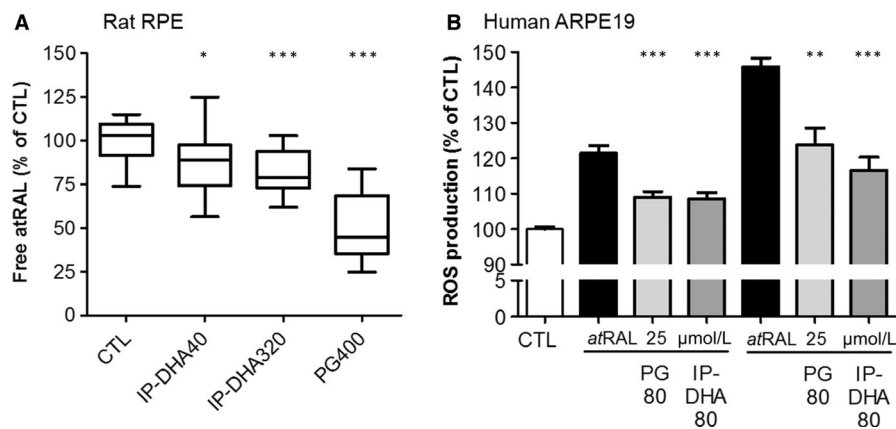


FIGURE 5 IP-DHA decreases free atRAL and prevents atRAL-induced ROS production in RPE. A, Primary rat RPE cells were cultured in 96-well plates, co-treated with 25 $\mu\text{mol/L}$ atRAL and 400 $\mu\text{mol/L}$ phloroglucinol (PG) or 40 and 320 $\mu\text{mol/L}$ IP-DHA for 4 h, and retinoids were extracted from cell lysates. The free atRAL content was quantified by HPLC from standard calibration. The data are from a representative experiment performed in triplicate and represented as mean \pm SD ($n = 3$). The data are expressed as a percentage of untreated cells (CTL). B, ARPE-19 cells were cultured in 96-well plates, pre-treated with 80 $\mu\text{mol/L}$ phloroglucinol (PG) or 80 $\mu\text{mol/L}$ IP-DHA for 24 h before incubation with H_2DCFDA for 30 min, and then, atRAL (25 or 50 $\mu\text{mol/L}$) was added for an additional 4 h. Fluorescent intensity was measured at $\lambda_{\text{em}} 535 \text{ nm}$ ($\lambda_{\text{exc}} = 485 \text{ nm}$) and expressed as a percentage of untreated cells (CTL). The data are expressed as mean \pm SEM ($n = 4$). * $P < .05$, ** $P < .01$, *** $P < .001$ vs atRAL-treated cells

outer retinal cells by scavenging ROS and trapping atRAL.⁹ However, a major disadvantage of phloroglucinol is its low bioavailability in the retina (unpublished personal data). Our strategy to improve selectivity for the retina relied on chemical modifications of the resorcinol core. We synthesized phloroglucinol derivatives by attaching DHA on a phenolic group. The choice of DHA was dictated by its high content in the photoreceptor disc membrane, the site of photoisomerization where atRAL is produced. Moreover, DHA has several advantages in the retina (a) it is avidly uptaken by RPE and retained in the POS,^{39,40} (b) it is essential for preserving visual functions and maintaining disc properties in the POS,⁴¹ (c) it facilitates the clearance of free retinal to prevent the accumulation of bisretinoid compounds associated within macular disease,⁴² and (d) it is a precursor of neuroprotectin D1 which protects the retina against oxidative stress induced by cell-injury-induced.⁴³ The second modification to phloroglucinol was the introduction of an isopropyl radical, whose electron-donating inductive effect should adjust the nucleophilicity of the aromatic ring to trap atRAL most efficiently.

Then, we evaluated the protective effect of IP-DHA against atRAL toxicity in outer retinal cells. IP-DHA was shown to be effective both in RPE and in NR. In the RPE, we showed that IP-DHA protects very well against atRAL compared to other lipophenols tested. IP-DHA and IP-LA are the most effective although at a different degree of unsaturation of PUFA. IP-C22 with a saturated C22 lipid chain has a very low efficiency comparable to that of phloroglucinol,¹³ showing the need for unsaturation in the fatty acid moiety. An explanation for this is an improvement in lipophilicity and an enhancement in cell permeability. We have shown in this study that the protective effect appears on the first hours of treatment and persists overtime, suggesting that lipophenol can be rapidly available and stabilized into the cell. The present data demonstrate that the PUFA grafting on alkylated phloroglucinol promotes survival of RPE cells.

Hence, we tried to elucidate further the mechanism of action of IP-DHA and compared its efficacy to that of phloroglucinol. Firstly, IP-DHA, but also phloroglucinol (albeit, at high concentration), efficiently reduces atRAL in primary cultures of rat RPE. Moreover, the production of ROS induced by atRAL and identified by H_2DCFDA is almost equally reduced by IP-DHA or by phloroglucinol. Together, these data suggest that IP-DHA and phloroglucinol are equally effective as anti-COS. However, as shown in our previous work,¹³ protection of ARPE-19 cells from atRAL toxicity by IP-DHA is four times greater than by phloroglucinol itself. We hypothesize that this could be due to: (a) a better bioavailability of IP-DHA due to high lipophilicity of DHA, and/or (b) the DHA fatty acyl chain that can promote the "direct reaction" (nucleophilic addition) of IP-DHA onto atRAL by lowering the activation energy required to scavenge atRAL and/or (c) IP-DHA triggering indirect cell defence enzyme systems. Cellular adducts between IP-DHA and atRAL have not yet been identified in vitro (chemical reaction and ARPE-19 incubation). By contrast, we were able to highlight the formation of retinal adducts with IP as a mixture of chromene-isopropyl (data not shown). We concluded that it was unlikely the presence of DHA would facilitate the reaction of IP-DHA on atRAL. The hypothesis that DHA improves cell bioavailability should be retained but requires further investigation by tracking IP-DHA into the cell. Interestingly, IP-DHA and IP-LA could be targeted rather than mitochondria where they could prevent atRAL from provoking ROS generation and COS in the RPE, thus protecting cells from apoptosis.^{3,44} The exact mechanisms of protection against atRAL toxicity are still unclear. The electron-donating inductive isopropyl ether group on phloroglucinol is necessary to increase its ability (electron enrichment of the aromatic ring) to protect against reactive electrophile atRAL.¹³ However, an additional role of the isopropyl function is

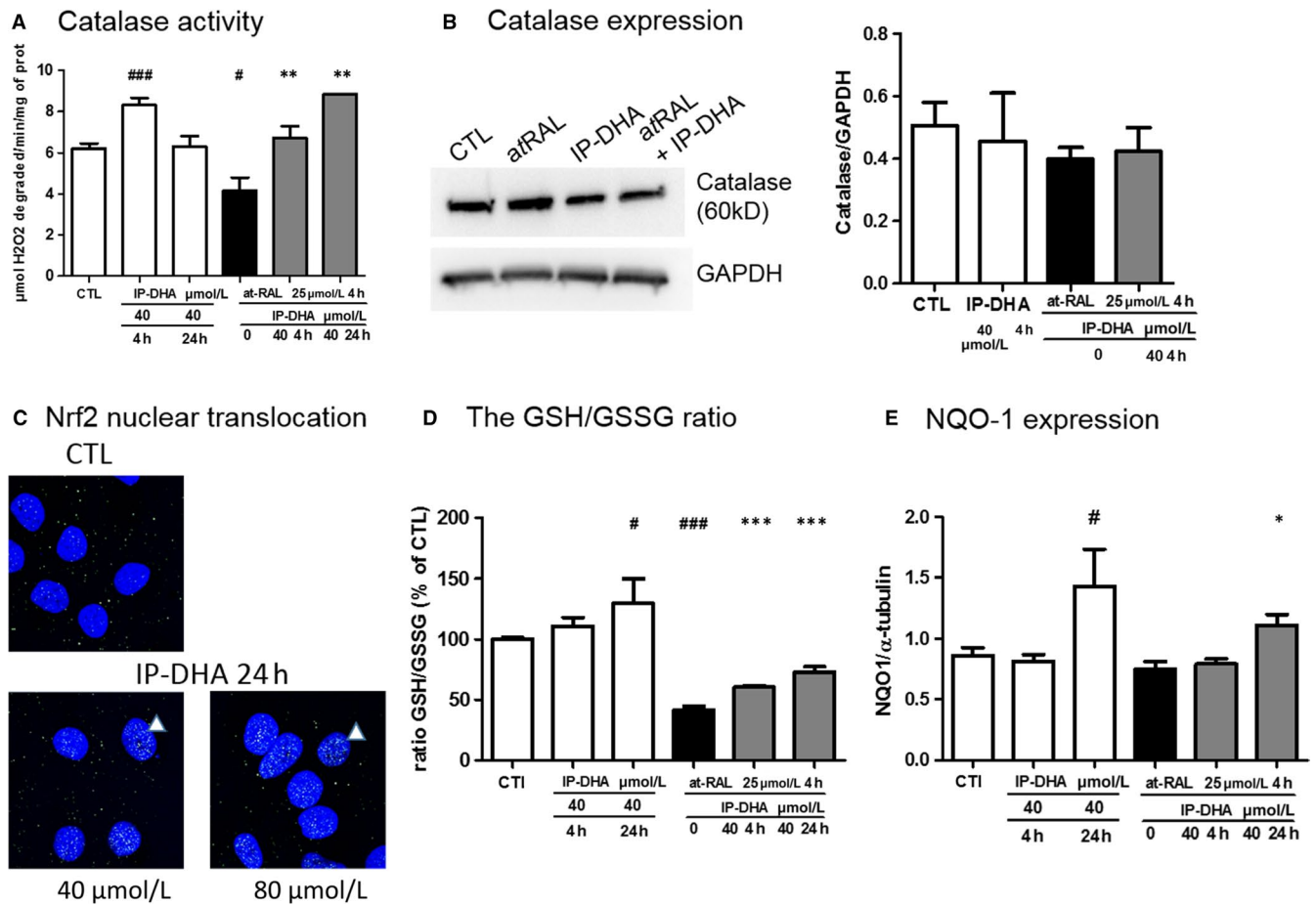


FIGURE 6 Effect of IP-DHA on antioxidant defence enzymes in ARPE-19. Effect of IP-DHA on antioxidant enzymes. Catalase activity (A) and its expression (B). ARPE-19 cells were incubated in 6-well plates for 4 h or 24 h with 40 µmol/L IP-DHA with or without 25 µmol/L atRAL during the last 4 h. Catalase activity was measured in cell lysates and expressed in µmol of H₂O₂ degraded/min/mg of protein. Catalase expression was quantified by Western blot analysis with a monoclonal rabbit anti-catalase antibody and enhanced chemiluminescence (ECL) detection using densitometry and ImageJ software. GAPDH expression was used as a loading control. Results are expressed as mean ± SEM (n ≥ 3). C, Nrf2 expression and nuclear translocation were explored by immunofluorescence with a rabbit monoclonal anti-Nrf2 antibody and Alexa488-conjugated anti-rabbit. Nuclei were stained with the blue fluorescent Hoechst dye. Confocal imaging revealed increased green spots in the nuclei after 24-h treatment with IP-DHA. Similar ARPE-19 treatments were performed, and GSH/GSSG ratio (D) and NQO-1 expression (E) were quantified. Results are expressed as mean ± SEM (n = 4). #P < .05, ###P < .001 vs untreated CTL and *P < .05, **P < .01, ***P < .001 vs atRAL-treated cells

not excluded, such as the steric hindrance in the vicinity of the DHA ester function that could protect it from esterase and improve the stability of the lipophenol. This latter point could not be established in this work, and it is not clear at present whether it could modulate the reactivity of phloroglucinol on atRAL. Further study is needed for elucidating the role of those two functions in more detail. Regarding reduction of oxidative status, we show that IP-DHA is able to up-regulate enzymatic responses in the short, as well as, in the long-term, by increasing the constitutive (catalase) or the inducible (Nrf₂-dependent Electrophilic Responsive Element (EpRE) pathway) enzymatic antioxidant activities, respectively. Thus, mechanism of action of IP-DHA may pass through direct ROS scavenging and/or by stimulating the production of several detoxifying enzymes of the EpRE through the transcription activity of Nrf2. Phloroglucinol itself has been described as being able to play a role in the antioxidant defences,

either directly (radical scavenging of ROS) or, more efficiently, by activating the Nrf2 pathway, in the case of a low level of oxidative stress.³⁷ With these latest results, it is possible to summarize the optimal characteristics of the chemicals showing the highest efficacy against STGD1, as well as the proven or most likely underlying mechanisms of action (table S2).

In the prospective treatment of patients with IP-DHA, we assume that the release of free DHA and IP may be part of the mechanism of action of the compound, as the ester bond could be cleaved by a plasma and/or cellular esterase. This is not a drawback as many studies show the beneficial effects of DHA supplementation in AMD and STGD1^{45,46} and dietary polyphenols in AMD against oxidative stress and beyond.⁴⁷ In addition, the oxidation of DHA not only causes deleterious effects (lipid peroxidation), but should also contribute to the release of cellular mediators (neuroprostane, neuroprotectin D1) helping the cell to fight oxidation. In addition, the

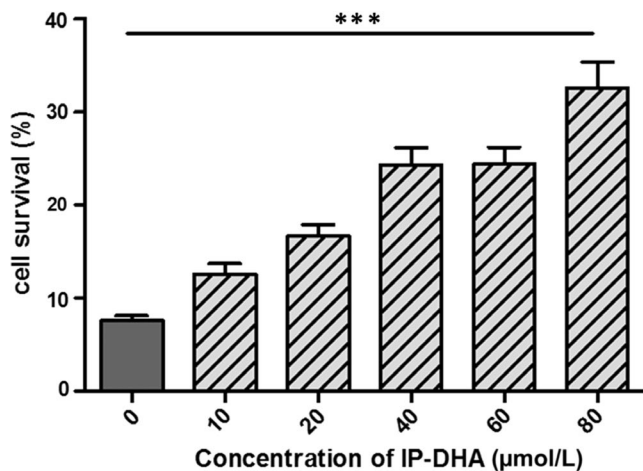


FIGURE 7 Protecting effect of IP-DHA against photo-oxidized A2E in ARPE-19. ARPE-19 cells were plated in 96-well plates (4×10^4 cells/well) and grown until confluency. Then, cells were untreated (grey bar) or treated with increasing doses of IP-DHA (hatched bars) for 1 h, prior to incubation with A2E (20 $\mu\text{mol/L}$) for 6 h. Cells were exposed to blue light (λ_{max} 430–470 nm, 4600 lux) and grown for 24 h before cell survival was determined by MTT assay. Data are expressed as a percentage of control untreated cells not exposed to A2E and are presented as mean \pm SD ($n = 3$ independent experiments). Unpaired Student's *t* test, $***P < .001$, non-treated vs exposed cells to photo-oxidized A2E. The maximum absorption of IP-DHA was 218 and 272 nm (see UV spectrum of IP-DHA in Supporting Information) which differs from that of blue light excitation (430–470 nm) and A2E maximum absorption (337–437 nm)

antioxidant activity of phloroglucinol would enhance the beneficial effect on vision.

In conclusion, our data show that IP-DHA is effective to protect outer retinal cells against lethal dose of atRAL. The beneficial role of IP-DHA in retinal cells involves both anti-carbonyl and anti-oxidative capacities. This suggests potential effects of lipophenols in the prevention of macular degeneration associated with COS, such as STGD1 and AMD. Additional studies will be necessary to examine the effect of IP-DHA in animal models of macular degeneration.

ACKNOWLEDGEMENTS

We would like to thank the ARPEGE Pharmacology Screening-Interactome platform for access to the xCELLigence system, Montpellier RIO Imaging for the use of imaging tools, and the Cellular Health Imaging Center of Clermont-Ferrand and C. Blavignac for help with flow cytometry. This research was supported in part by grant from Fondation Stargardt, under the aegis of Fondation Valentin Hauy, and Retina France (no 2017-03). We also thank Inserm, CNRS and University of Montpellier for their support. The authors are grateful to Dr Vasiliki Kalatzis and Dr Patrick Carroll for their assistance in English language editing.

CONFLICT OF INTEREST

The authors have declared that no conflict of interest exists.

AUTHORS CONTRIBUTIONS

AC, EM, LG, NJ, MR and CA-P. conducted the experiments; AC, DC, CC and PB designed the research studies; AC, EM, DC, CA-P. and PB acquired and analysed data; PB prepared the published work and wrote the initial draft; DC, CC and JV reviewed and improved the manuscript; GL, TD and PB acquired financial support for the project; JV, CC and PB supervised the research activity; and IM coordinated the Centre for Inherited Sensory Disorders.

DATA AVAILABILITY STATEMENT

The data that support the findings of this study are available from the corresponding author upon reasonable request.

ORCID

Philippe Brabet  <https://orcid.org/0000-0003-2739-1622>

REFERENCES

- Palczewski K. Chemistry and biology of vision. *J Biol Chem.* 2012;287:1612-1619.
- Kiser PD, Golczak M, Palczewski K. Chemistry of the retinoid (visual) cycle. *Chem Rev.* 2014;114:194-232.
- Maeda A, Maeda T, Golczak M, et al. Involvement of all-trans-retinal in acute light-induced retinopathy of mice. *J Biol Chem.* 2009;284:15173-15183.
- Shroyer NF, Lewis RA, Allikmets R, et al. The rod photoreceptor ATP-binding cassette transporter gene, ABCR, and retinal disease: from monogenic to multifactorial. *Vision Res.* 1999;39:2537-2544.
- Chen Y, Okano K, Maeda T, et al. Mechanism of all-trans-retinal toxicity with implications for stargardt disease and age-related macular degeneration. *J Biol Chem.* 2012;287:5059-5069.
- Sawada O, Perusek L, Kohno H, et al. All-trans-retinal induces Bax activation via DNA damage to mediate retinal cell apoptosis. *Exp Eye Res.* 2014;123:27-36.
- Li J, Cai X, Xia Q, et al. Involvement of endoplasmic reticulum stress in all-trans-retinal-induced retinal pigment epithelium degeneration. *Toxicol Sci.* 2015;143:196-208.
- Zhu X, Wang KE, Zhang K, Zhou F, Zhu L. Induction of oxidative and nitrosative stresses in human retinal pigment epithelial cells by all-trans-retinal. *Exp Cell Res.* 2016;348:87-94.
- Cia D, Cubizolle A, Crauste C, et al. Phloroglucinol protects retinal pigment epithelium and photoreceptor against all-trans-retinal-induced toxicity and inhibits A2E formation. *J Cell Mol Med.* 2016;20:1651-1663.
- Nickell S, Park PS, Baumeister W, Palczewski K. Three-dimensional architecture of murine rod outer segments determined by cryoelectron tomography. *J Cell Biol.* 2007;177:917-925.
- Masutomi K, Chen C, Nakatani K, Koutalos Y. All-trans retinal mediates light-induced oxidation in single living rod photoreceptors. *Photochem Photobiol.* 2012;88:1356-1361.
- Liu J, Itagaki Y, Ben-Shabat S, Nakanishi K, Sparrow JR. The biosynthesis of A2E, a fluorophore of aging retina, involves the formation of the precursor, A2-PE, in the photoreceptor outer segment membrane. *J Biol Chem.* 2000;275:29354-29360.
- Crauste C, Vigor C, Brabet P, et al. Synthesis and evaluation of polyunsaturated fatty acid-phenol conjugates as anti-carbonyl-stress lipophenols. *Eur J Organ Chem.* 2014;2014:4548-4561.
- Kim SR, Jang YP, Jockusch S, Fishkin NE, Turro NJ, Sparrow JR. The all-trans-retinal dimer series of lipofuscin pigments in retinal pigment epithelial cells in a recessive Stargardt disease model. *Proc Natl Acad Sci USA.* 2007;104:19273-19278.

15. Ueda K, Zhao J, Kim HJ, Sparrow JR. Photodegradation of retinal bisretinoids in mouse models and implications for macular degeneration. *Proc Natl Acad Sci USA*. 2016;113:6904-6909.
16. Zhou J, Ueda K, Zhao J, Sparrow JR. Correlations between photodegradation of bisretinoid constituents of retina and dicarbonyl adduct deposition. *J Biol Chem*. 2015;290:27215-27227.
17. Pinteá A, Rugina D, Pop R, et al. Antioxidant effect of trans-resveratrol in cultured human retinal pigment epithelial cells. *J Ocul Pharmacol Ther*. 2011;27:315-321.
18. Zhu Q, Zheng ZP, Cheng KW, et al. Natural polyphenols as direct trapping agents of lipid peroxidation-derived acrolein and 4-hydroxy-trans-2-nonenal. *Chem Res Toxicol*. 2009;22:1721-1727.
19. Parish CA, Hashimoto M, Nakanishi K, Dillon J, Sparrow J. Isolation and one-step preparation of A2E and iso-A2E, fluorophores from human retinal pigment epithelium. *Proc Natl Acad Sci USA*. 1998;95:14609-14613.
20. Marie M, Bigot K, Angebault C, et al. Light action spectrum on oxidative stress and mitochondrial damage in A2E-loaded retinal pigment epithelium cells. *Cell Death Dis*. 2018;9: Article number 287.
21. Angebault C, Gueguen N, Desquiret-Dumas V, et al. Idebenone increases mitochondrial complex I activity in fibroblasts from LHON patients while producing contradictory effects on respiration. *BMC Res Notes*. 2011;4:Article number 557.
22. Loiseau D, Chevrollier A, Verry C, et al. Mitochondrial coupling defect in Charcot-Marie-Tooth type 2A disease. *Ann Neurol*. 2007;61:315-323.
23. Benit P, Slama A, Rustin P. Decylubiquinol impedes mitochondrial respiratory chain complex I activity. *Mol Cell Biochem*. 2008;314:45-50.
24. James AM, Wei YH, Pang CY, Murphy MP. Altered mitochondrial function in fibroblasts containing MELAS or MERRF mitochondrial DNA mutations. *Biochem J*. 1996;318(Pt 2):401-407.
25. Rustin P, Chretien D, Bourgeron T, et al. Assessment of the mitochondrial respiratory chain. *Lancet*. 1991;338:60.
26. Schulman JD, Blass JP. Measurement of citrate synthase activity in human fibroblasts. *Clin Chim Acta*. 1971;33:467-469.
27. Halliwell B, Whiteman M. Measuring reactive species and oxidative damage in vivo and in cell culture: how should you do it and what do the results mean? *Br J Pharmacol*. 2004;142:231-255.
28. Gegotek A, Skrzydlewska E. Biological effect of protein modifications by lipid peroxidation products. *Chem Phys Lipids*. 2019;221:46-52.
29. Ergin V, Hariry RE, Karasu C. Carbonyl stress in aging process: role of vitamins and phytochemicals as redox regulators. *Aging Dis*. 2013;4:276-294.
30. Inoue Y, Shimazawa M, Noda Y, et al. RS9, a novel Nrf2 activator, attenuates light-induced death of cells of photoreceptor cells and Muller glia cells. *J Neurochem*. 2017;141:750-765.
31. Turrens JF. Mitochondrial formation of reactive oxygen species. *J Physiol*. 2003;552:335-344.
32. Zou X, Gao J, Zheng Y, et al. Zeaxanthin induces Nrf2-mediated phase II enzymes in protection of cell death. *Cell Death Dis*. 2014;5:e1218.
33. Sparrow JR, Gregory-Roberts E, Yamamoto K, et al. The bisretinoids of retinal pigment epithelium. *Prog Retin Eye Res*. 2012;31:121-135.
34. Sparrow JR, Wu Y, Kim CY, Zhou J. Phospholipid meets all-trans-retinal: the making of RPE bisretinoids. *J Lipid Res*. 2010;51:247-261.
35. Bhullar KS, Rupasinghe HP. Polyphenols: multipotent therapeutic agents in neurodegenerative diseases. *Oxid Med Cell Longev*. 2013;2013:891748.
36. Pérez-Hernández J, Zaldívar-Machorro VJ, Villanueva-Porras D, Vega-Ávila E, Chavarría A. A potential alternative against neurodegenerative diseases: phytodrugs. *Oxid Med Cell Longev*. 2016;2016:8378613.
37. Ryu J, Zhang R, Hong B-H, et al. Phloroglucinol attenuates motor functional deficits in an animal model of Parkinson's disease by enhancing Nrf2 activity. *PLoS One*. 2013;8:e71178.
38. Yang E-J, Ahn S, Ryu J, et al. Phloroglucinol attenuates the cognitive deficits of the 5XFAD mouse model of Alzheimer's Disease. *PLoS One*. 2015;10:e0135686.
39. Wang N, Anderson RE. Transport of 22:6n-3 in the plasma and uptake into retinal pigment epithelium and retina. *Exp Eye Res*. 1993;57:225-233.
40. Rice DS, Calandria JM, Gordon WC, et al. Adiponectin receptor 1 conserves docosahexaenoic acid and promotes photoreceptor cell survival. *Nat Commun*. 2015;6:Article number 6228.
41. Shindou H, Koso H, Sasaki J, et al. Docosahexaenoic acid preserves visual function by maintaining correct disc morphology in retinal photoreceptor cells. *J Biol Chem*. 2017;292:12054-12064.
42. Dornstauder B, Suh M, Kuny S, et al. Dietary docosahexaenoic acid supplementation prevents age-related functional losses and A2E accumulation in the retina. *Invest Ophthalmol Vis Sci*. 2012;53:2256-2265.
43. Mukherjee PK, Marcheselli VL, Serhan CN, Bazan NG. Neuroprotectin D1: a docosahexaenoic acid-derived docosatriene protects human retinal pigment epithelial cells from oxidative stress. *Proc Natl Acad Sci USA*. 2004;101:8491-8496.
44. O'Connell KA, Dabkowski ER, de Fatima GT, et al. Dietary saturated fat and docosahexaenoic acid differentially effect cardiac mitochondrial phospholipid fatty acyl composition and Ca(2+) uptake, without altering permeability transition or left ventricular function. *Physiol Rep*. 2013;1:e00009.
45. Georgiou T, Neokleous A, Nicolaou D, Sears B. Pilot study for treating dry age-related macular degeneration (AMD) with high-dose omega-3 fatty acids. *PharmaNutrition*. 2014;2:8-11.
46. Querques G, Benlian P, Chanu B, et al. DHA supplementation for late onset Stargardt disease: NAT-3 study. *Clin Ophthalmol*. 2010;4:575-580.
47. Pawlowska E, Szczepanska J, Koskela A, Kaarniranta K, Blasiak J. Dietary polyphenols in age-related macular degeneration: protection against oxidative stress and beyond. *Oxid Med Cell Longev*. 2019;2019:9682318.
48. Liu Y, Zhang D, Wu Y, Ji B. Docosahexaenoic acid aggravates photo-oxidative damage in retinal pigment epithelial cells via lipid peroxidation. *J Photochem Photobiol B*. 2014;140:85-93.

SUPPORTING INFORMATION

Additional supporting information may be found online in the Supporting Information section.

How to cite this article: Cubizolle A, Cia D, Moine E, et al. Isopropyl-phloroglucinol-DHA protects outer retinal cells against lethal dose of all-trans-retinal. *J Cell Mol Med*. 2020;24:5057-5069. <https://doi.org/10.1111/jcmm.15135>